2009

The effect of spring restraint on weld distortion in t-joint fillet welds

Michael A. Rickers
Iowa State University

The effect of spring restraint on weld distortion in t-joint fillet welds

by

Michael A. Rickers

A thesis submitted to the graduate faculty

in partial fulfillment of the requirements for the degree of

MASTER OF SCIENCE

Major: Industrial Engineering

Program of Study Committee:
Frank E. Peters, Major Professor
Matthew C. Frank
L. Scott Chumbley

Iowa State University

Ames, Iowa

2009

Table of Contents

List of Figures

Acknowledgements

I would like thank my major professor Dr. Frank Peters for all his support and direction throughout this research project. I would also like to thank my other graduate committee members, Dr. Matt Frank and Dr. Scott Chumbley for being my committee members. Special thanks goes to Kevin Brownfield for all his help with fixture design and much more and also to Zhongyuan Qian for his help with x-ray diffraction measurements.

A special thanks also to Mike Boyd at John Deere Des Moines Works in Ankeny, Iowa first for allowing me to come to their facility and secondly for producing several weldments for me. This project greatly benefited from his involvement.

Lastly, I would like to thank my family for all their support over the entirety of my time here at Iowa State University.

Abstract

T-joint fillet welds are a very common occurrence found in industry today. Localized heating and cooling from the welding process lead to the rise of distortion and residual stresses. Weld fixturing is a common practice in industry used to address the problems associated with welding, however fixturing also creates problems of residual stresses being locked into the weldment. This research involves placing linear compression springs along the top of a t-joint fillet weld in an effort to gain an understanding of the contraction of the weld metal. The effect of different levels of restraint is also investigated. Variable restraint is a concept that could be used to reduce distortion while keeping residual stress at a minimal level. The idea behind this is that unnecessary force applied to a part could leave stress in that part; variable restraint would use force where it is needed. Residual stresses were obtained for the weldments by the x-ray diffraction process. The distortion and stress trends are presented and discussed in this work.

Chapter 1. Introduction

Arc welding is one of the most common welding processes used in industry today, mainly due to its versatility and relatively low cost. The particular arc welding process used in this investigation is gas metal arc welding, or GMAW. While welding is a very useful process with many advantages, there are distinctive problems that arise because of the complexity of welding. Residual stresses and distortion are two that play an important role in the design process of welded structures.

Welding distortion can be attributed to rapid heating and cooling in localized regions of the workpiece during welding resulting in thermal expansion and contraction, and thus distortion [1]. Weld deformation can fall under different types including: transverse shrinkage, rotational distortion, angular distortion, longitudinal bending, longitudinal shrinkage, and buckling distortion. Figure 1 shows examples of each type of distortion. Transverse shrinkage is shrinkage that is perpendicular to the weld line, and longitudinal shrinkage occurs parallel to the weld line. Rotational distortion is deformation in the plane of the plate usually attributed to the weld being off of the neutral axis. Angular distortion is can be described as a rotation of the piece about the weld line because of the non-uniform thermal gradients in the welding process. Longitudinal bending distortion occurs in a plane perpendicular to the weld line, the plate bends down the length of the plate. Although the method in this research prevents more than just one type of distortion, longitudinal bending will be the main distortion that is investigated in this paper because the data closely resembles longitudinal bending.

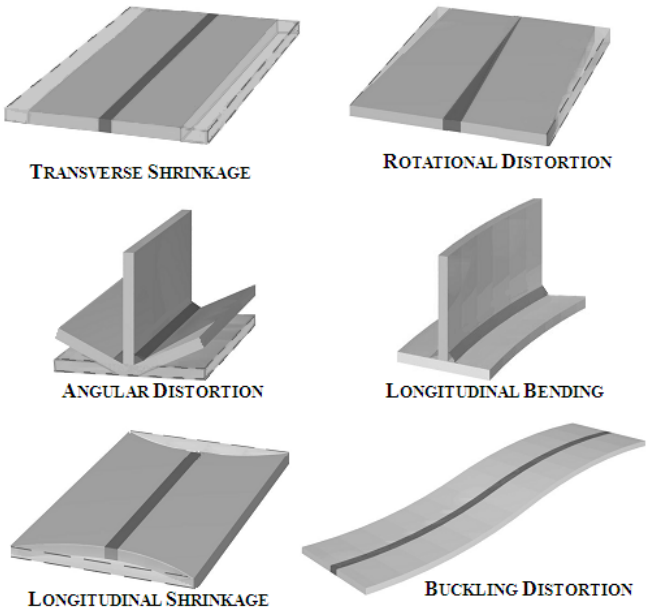

Figure 1. Types of Welding Distortion [2]

Welding shrinkage cannot be fully prevented, but it can be controlled. Distortion reduction is fundamental in efforts to overcome weld distortion. Some methods that are used to control distortion include: pre-straining, pre-setting, pre-heating, as well as more common solutions such as intermittent welding, sequencing, and using the correct amount of weld. Masubuchi used pre-heating to control the longitudinal distortion in welding [3]. Specifically, Masubuchi created an in process control to reduce joint mismatch in butt welds and also to reduce longitudinal bending distortion in built up beams. For the limited case study he performed, his results were positive, allowing distortion to be reduced to near zero with the correct heating conditions. Kumose and Yoshida investigated the effects of plastic and elastic pre-straining to avoid distortion [4]. Pre-straining involves bending the plate either plastically or elastically in the opposite direction of the expected distortion due to welding. Pre-setting involves placing pieces in such a way that they will move into the desired position after welding is completed. Pre-setting accounts for the shrinkage that occurs from welding to minimize distortion.

Welding fixtures are used to hold two or more parts together while they are being joined. It is also a very common practice in industry to reduce distortion caused by welding by using fixtures, in addition to holding the parts. Fixture design is a common challenge in industry due to the complexity of the welding process. To add to this complexity, weld assemblies rely on the accuracy of the weld fixture to properly align parts, and also must be able to withstand the heat of the welding process without distortion and without dissipating heat away from the weld. While fixturing may solve the distortion problem, it creates another. By restraining the part against movement in the welding process, residual stresses are built up within that part because of the restraint. Withers and Bhadeshia describe residual stress as stress that remains in a body that is stationary and at equilibrium with its surroundings. It can be very detrimental to the performance of a material or the life of a component [5]. Because of the complexity of the welding process, it is almost certain that the force required to fixture a part during welding will not be identical across the entirety of the part. Variable restraint is a concept that could be used to reduce distortion while keeping residual stress at a minimal level. The idea behind this is that unnecessary force applied to a part could leave stress in that part; variable restraint would use force where it is needed.

The goal of this study is to obtain distortion and residual stress data to be used to understand the contracting metal in the weld bead, as well as the effect of restraint on the contracting metal. This will be accomplished by performing weld trials and assessing the distortion data using physical properties of steel. Linear springs will be used as restraint in this experiment. A relationship between distortion and residual stress at different levels of restraint will be determined. The scope of this model is limited to t-joint fillet welds.

Chapter 2. Literature Review

A search of research literature was performed for information associated with welding distortion prediction. A brief overview of work done on estimating the heat distribution of the welding process will be done. Previous work with residual stress and distortion in welding will be a main focus of this literature review. A discussion of previous work done on the effect of restrained contraction in steel castings will be presented. Restrained contraction in steel castings was investigated due to the similarities between the welding and casting processes; molten metal cooling and contracting is present in both processes.

The problems of distortion and residual stress in a welded joint can be directly attributed to the thermal aspect of the welding process, most specifically the rapid heating and localized concentrated heat input that the weld joint experiences. One researcher to describe the theory behind the heat distribution in welding was Rosenthal. Rosenthal applied Fourier heat flow theory to moving heat sources [6]. What came from his research was an analytical method of modeling the welding heat source as either a point, line, or a plane. While this is still a popular method of calculating the thermal history of a weld, it has been found ineffective in estimating the thermal behavior of the weld pool. Since then, a number of researchers have looked into the modeling the welding heat source with different concepts of the source and heat distribution to find a better estimation. Goldak proposed a new mathematical model for weld heat sources based on a Gaussian distribution of power in 1984 [7]. Goldak proposes that the welding heat source be modeled as a double ellipsoid configuration. The double ellipsoid heat source overcomes the limitation of previous heat source models that there are two separate and different temperature gradients. The front half of the source is a quadrant of one ellipsoid, and the rear half is a quadrant of another ellipsoid. Figure 2 shows the double ellipsoid heat source configuration. Goldak's new method has been shown to be more accurate than previous methods such as the Pavelic disc method, as well as the previously mentioned Rosenthal theory for heat distribution in welding.

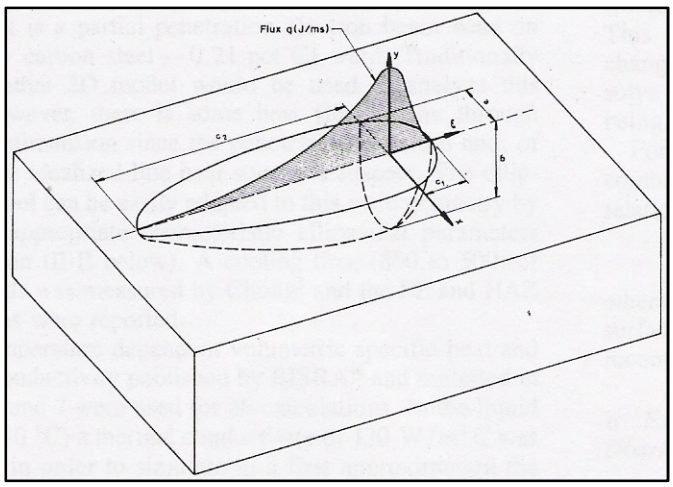

Figure 2. Double ellipsoid heat source configuration of Goldak [7]

Although Goldak has a good method, there was not an analytical solution until Nguyen came up with one in 1999. Nguyen came up with analytical solutions for the transient temperature field for a double ellipsoidal heat source and experimentally verified his findings [8]. Good agreement between numerical and experimental results shows the credibility of these solutions and thus a great potential to be applied in thermal and residual stress analysis and calculations. Knowledge of the heat source and its effect on the weld specimen is important to know to understand the welding process as a whole and where the problems of distortion and residual stress are coming from.

There are many ways to control welding distortion, as discussed earlier. This section of the literature review will discuss previous work done in controlling and predicting distortion caused by welding. Tsai introduced a spring-shrinkage model to predict the distortion from welding in butt and tee joint welded structures [9]. In Tsai's model, he used a series of spring elements along the welds to acquire the equivalent shrinkage force created by the weld. The spring properties used by Tsai were spring constant and spring force, which were required to develop the equivalent conditions. After developing the theoretical properties, the spring-shrinkage model was tested for applicability, resulting in good agreement between theoretical and experimental results. A limitation of this research is the lack of a physical experiment. The applicability study performed was a finite element model incorporating Tsai's spring-shrinkage model into the model. Although models are created to predict distortion and residual stresses, a physical experiment would better confirm that the model proposed is accurate.

Mahapatra et al. 2006 investigated the use of constraint in one-side fillet welding to see its effect on angular distortion [10]. Strategically placed tack welds were used to counter the effect of the welding process. Results of the experiment showed that applying constraints at the proper position could indeed counter the distortion from welding. However, no study of residual stress was included in this

investigation. Similar to Mahapatra, Kumose et al. 1954 looked into prediction of angular distortion in one-pass fillet welding [11]. Pre-straining to eliminate distortion in welding was researched. Pre-straining involves either plastic or elastic straining in the direction opposite to distortion before welding is done. Figure 2 below shows an example of elastic pre-strain.

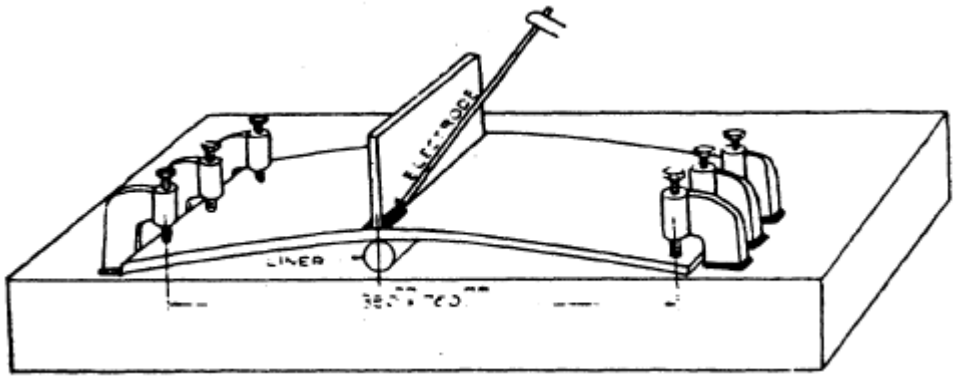

Figure 3. Elastic pre-straining example [11]

Kumose found that the magnitude of plastic pre-strain to avoid distortion was comparatively smaller than that of free angular distortion when the flange thickness is comparatively greater than the weld leg length. Free angular distortion in this research is referring to angular distortion that is free from external forces and only affected by the experimental parameters. When applying elastic pre-strain to a welded component, Kumose found that it was only necessary to consider applied skin stress and nothing else to find suitable values to avoid distortion, meaning that skin stress is directly related to amount of distortion.

Michaleris investigated the use of the thermal tensioning technique to reduce residual stress and distortion in welding [12]. Thermal tensioning is pre-heating of the weldment before the welding takes place. He proposes the use of heating bands which move along with the torch on either side of the weld. Thermal tensioning works to control residual stress and distortion by generating a tensile strain and the weld zone prior to and during welding by imposing a temperature differential. The width and length of the band are obtained by optimization of the parameters that would lead to minimal stress and distortion.

Okerblom laid the groundwork for simplified analytical models of the welding process [13]. He proposed a model that predicted the curvature and contraction (shrinkage) of longitudinal bending distortion in t-joint fillet welds. Figure 4 shows examples of longitudinal bending and longitudinal contraction.

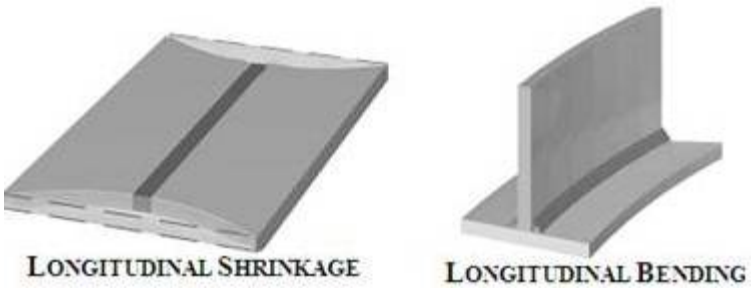

Figure 4. Longitudinal bending and contraction [2]

Using simple elasticity and plasticity theory, he determined magnitude of curvature and contraction based on heat input from the welding process, the center of gravity of the weldment, and the basic material properties of carbon steel such as thermal expansion and yield stress. He also identified that the major permanent deformations are driven by the cooling phase of the welding process. That fact is what allowed him to use a simple treatment for the longitudinal contraction previously discuss. An analytical method that came about from Okerblom's simplifications was the mismatched thermal strain method (MTS).

Camilleri et al. 2005 extended Okerblom's work on longitudinal welding deformations [14]. Of interest in his work is the contraction force that he derived. The total force generated by the contracting weld metal is represented by the cross-hatched area in Figure 5 below.

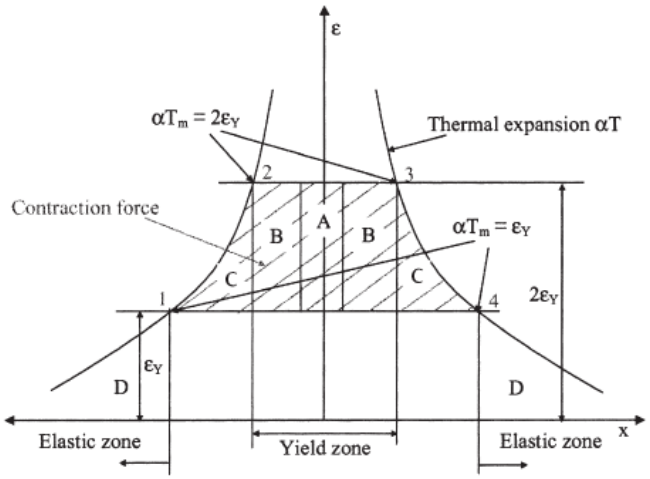

Figure 5. Formulation of total contraction force via MTS [14]

If the force is integrated over the area, an equation for the force can be provided as a relationship between heat input and material properties, as shown below in Equation 1, Camilleri et al. 2005. His results show that the critical controlling parameter on longitudinal contraction force is the heat input rate, which is well known. Also the result is independent of yield strength.

$$F = 0.335 \frac{q}{v} \frac{\alpha}{c\rho} E \quad (1)$$

Residual stresses due to the welding process are inevitable and their effects on welded components cannot be ignored. This section of the literature review will discuss the previous work done in measuring residual stresses as well as the effect of residual stresses in welding. Teng et al. 1998 investigated the effect of weld conditions on residual stresses in butt welds [15]. He predicted residual stresses in one pass arc welding using the finite element package ANSYS. As stated before, Teng was using butt welded steel plates, and was predicting both the longitudinal and transverse residual stresses. He used spacing between stress points of roughly 10 millimeters for the longitudinal stress (parallel to weld line) and a spacing of roughly 15 millimeters for the transverse stress (perpendicular to weld line). Teng did not specify where these points occur, but it is assumed that they are on the surface of the steel plate. Figure 6 shows the transverse residual stress along the direction of the weld line. Figure 7 shows the transverse residual stress perpendicular to the weld direction.

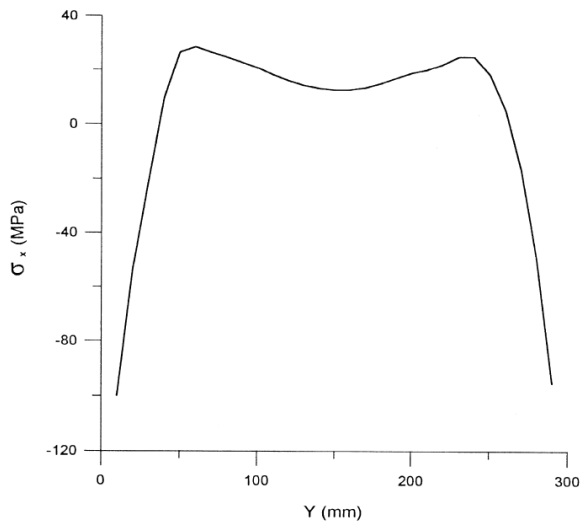

Figure 6. Transverse stress parallel to weld line [15]

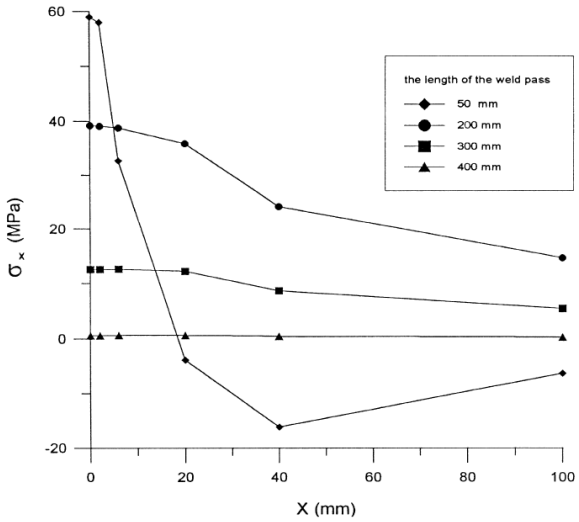

Figure 7. Transverse stress perpendicular to weld line [15]

The main conclusion taken from this investigation was that the magnitude of the residual stresses with a restrained joint is larger than Teng estimated with that of an unrestrained joint. Similarly, Teng et al. 2001 was an analysis into residual stresses specifically in t-joint fillet welds [16]. Residual stresses were again predicted with a finite element method, and it was assumed that both sides of the t-joint were welded simultaneously. Spacing between stress points of roughly 3 millimeters was used for both the longitudinal stress and for the transverse stress. The stress points are located on the surface of the base plates of the t-joint. Teng briefly investigates the effect of restraint on angular distortion and residual stresses near the toe of the weld. He found that the peak residual stress was decreased with restraint and he showed that the technique used to prevent angular distortion also reduced stress near the toe of the weld. Figure 8 shows the transverse stress perpendicular to the weld line.

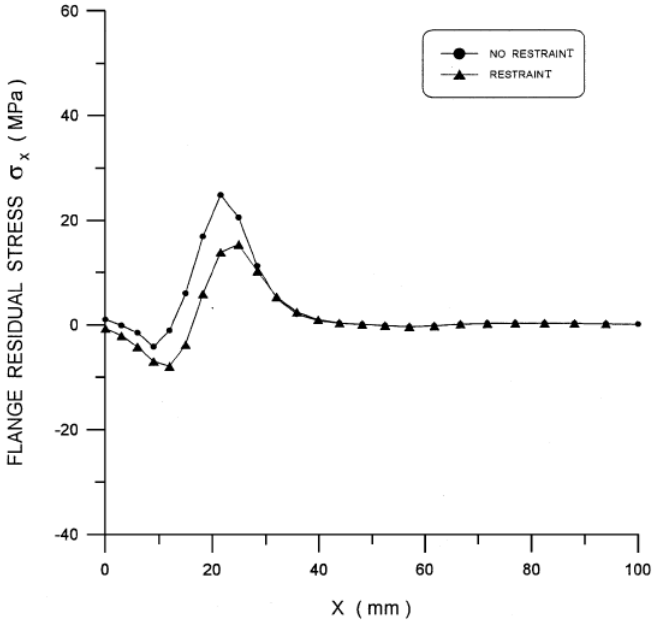

Figure 8. Transverse residual stress perpendicular to weld line [16]

Tekriwal et al. 1991 used ABAQUS finite element software to predict residual stress distributions in v-groove butt welded plates [17]. Tekriwal found that the maximum transverse stress is produced near the heat-affected zone (HAZ) boundary. Andersson looked at the transverse stress in butt welded joints done by submerged arc welding [18]. The stress points are located on both the top and bottom surfaces of the plates. Andersson used strain gages to capture the stress data from the welding process. Figure 9 below shows a picture of the strain gage setup on the butt welded plates.

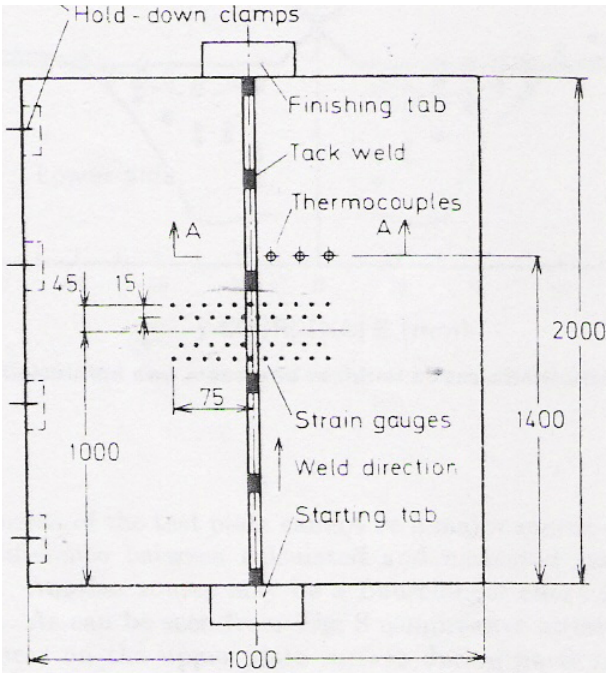

Figure 9. Arrangement for strain gages for stress analysis in butt welded plates. [18]

Andersson found that the hold down clamps were giving additional restraining forces of 10-25 MPa that added tensile stress to the strain gage measurements, which is in-line with other papers in saying that restraint increases residual stresses.

Wimpory et al. 2003 did a study examining the measurement of residual stresses in t-plate weldments [19]. Neutron diffraction was the method used to obtain the residual stresses for these t-joint weldments. The measurements were taken at the toe of the weld through the thickness of the base plate. Spacing between these measurements was roughly 1 millimeter, both in the longitudinal and transverse directions. Figure 10 below shows the typical sample done for this experiment.

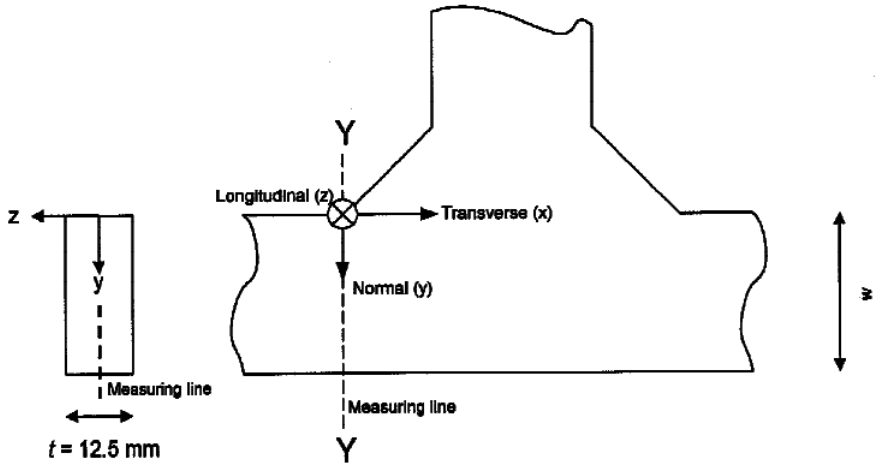

Figure 10. T-plate weld with measurement directions indicated. [19]

Wimpory found that the residual stress distribution had a maximum tensile value of 120 ± 20 MPa close to the weld toe, which is similar to what Tekriwal found with the HAZ boundary being the highest stress value.

After an extensive search of welding literature did not reveal any methods a priori, restrained contraction in steel castings was investigated due to the similarities between the welding and casting processes; molten metal cooling and contracting is present in both processes. An extensive study on the solidification behavior of steel castings was performed by Briggs between 1933 and 1936. This series of investigations covered everything from formation of hot tears to contraction stresses of steel. Briggs' second installation of the study was interesting and applied directly to this research. In the second installation, Briggs performed a study on hindered contraction in steel castings for varying levels of restraint [20]. One of the topics that Briggs wanted to answer with this study was the comparison of the loads in free contraction versus hindered contraction. The test casting used by Briggs was a round bar made in green sand. The bar design was important to obtain a uniform cooling rate through the entire casting for the sake of accuracy of data. The bar was developed with large ends and a smaller central

section to achieve the desired uniform cooling rate and eliminate problems of contraction and expansion occurring simultaneously. Figure 11 below shows Briggs' bar design.

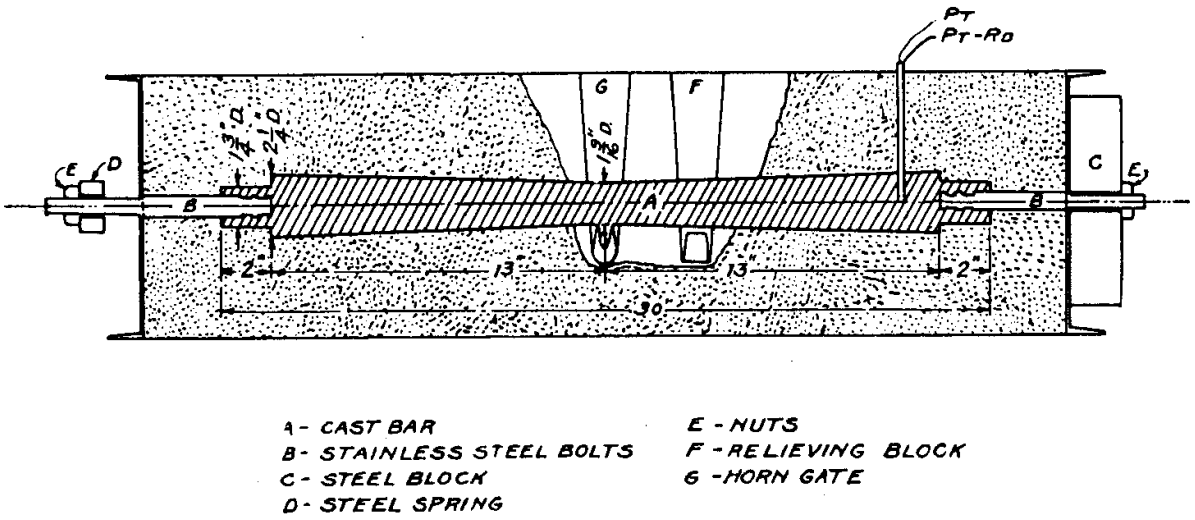

Figure 11. Design of contraction bar [20]

The bar was secured to the outside of the mold on one side and fastened to a flat steel spring on the other side. Steel springs were used to restrain the contraction of the steel during cooling; they were used to cause tensions similar to those that would be encountered by castings. Three different springs were used to provide three different levels of restraint to be measured. Briggs could then study the effect of the restraint of the different springs on the contraction of the steel. Figure 12 is a graph of the amount of contraction versus the solidification time for the three levels of spring restraint, as well as the free contraction trial. As is clear in Figure 12, the amount of contraction experienced by the bar decreases with increased restraint from the springs. A practical use that Briggs states for the data is to determine the amount of stress a particular casting has encountered by measuring the pattern and casting to find amount of contraction and hence the amount of stress. Briggs' data makes it possible to find a stress level at a certain temperature of the cooling steel, which is very useful in determining the strength of steel around its melting point. This research performed by Briggs is the basis for experiment performed in this study.

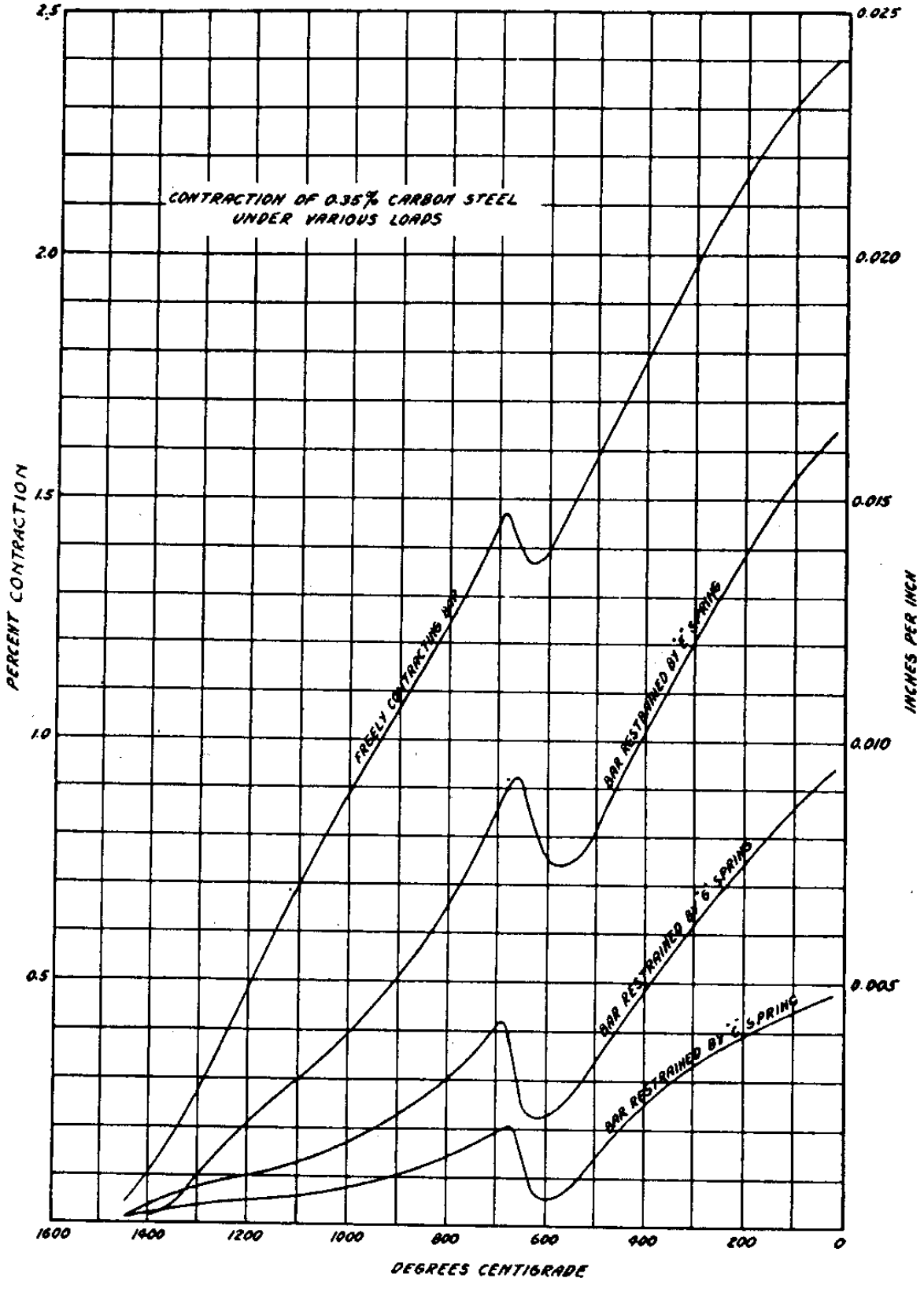

Figure 12. Contraction of 0.35% carbon steel under various loads [20]

A review of the literature related to this subject has revealed many different methods of analyzing residual stress and distortion in welding, but nothing is found a priori to the method of this research. The research discussed throughout this paper involves using linear springs to restrain a t-joint fillet weld as a method of reducing distortion and residual stress, while investigating what effect the restraint has on the contracting weld metal. This will be discussed in much greater detail in the next section of this paper. The knowledge acquired during this search was instrumental in forming the direction of this project

Chapter 3. Experimental Setup

The objective of the experiments is to understand the relationship between distortion, residual stress, and restraint. This is achieved by obtaining distortion and stress data described in the following chapter.

Two AISI 1018 steel plates, one with dimensions 12” x 3” x 3/8” (base plate) and another with dimensions 12” x 4” x 3/8” (vertical plate), were welded together in a one pass “T” joint using the gas metal arc welding process (GMAW) as shown in Figure 13 below.

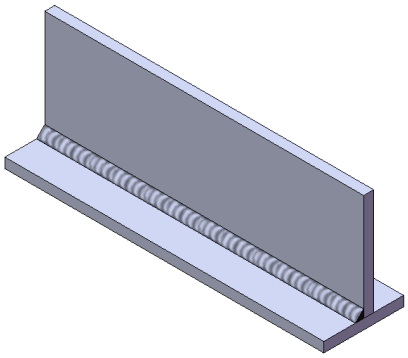

Figure 13. One pass t-joint fillet weld

Variables that affect the weld bead and were controlled in this setup include, but are not limited to, voltage, amperage, and wire speed. The Procedure Handbook for Arc Welding was referenced to find the recommended combination of variables for the type of material and joint used in this research [21]. From the recommendations of the handbook and a few trial welds, the weld settings for this experiment were determined and are shown in Table 1 below.

Table 1. Weld Parameter Settings

Voltage (V)	Amperage (A)	Wire Speed (in. /min.)	Travel Speed (in. /min.)
28	335	475	13

A fixture was used to hold the part which is described below. Since the goal of this experiment was to understand the contracting weld metal, linear compression springs were used to attain said goal. These springs were placed across the top edge of the t-joint to act as a restraint to the contraction of the weld metal, resisting distortion that occurs due to the welding process. The springs were placed every 2 inches across the top of the vertical piece of the t-joint for a total of 6 springs across the entire weldment. Several different levels of spring restraint were tested in this experiment and will be discussed in more detail later on in this section.

A weld fixture needed to be created to hold the springs in placed on the weldment during the welding process. It needed to allow access to the weld along with being able to hold the springs in place and allowing measurements to be taken all without removing the weldment or unclamping it. Figure 14 shows the weldment loaded into a weld fixture created to hold it while the welding occurs. The bottom plate was clamped down to the fixture to allow the distortion to be reflected in the vertical piece of the t-joint. Two plate clamps were used along the bottom plate on the back side of the weldment and two bolts were used to clamp the bottom plate on the weld side to allow the weld gun access to the weld joint. Tack welds on each end of the weldment were used to hold the vertical piece in the case where no springs were present and the springs hold the vertical piece in other cases.

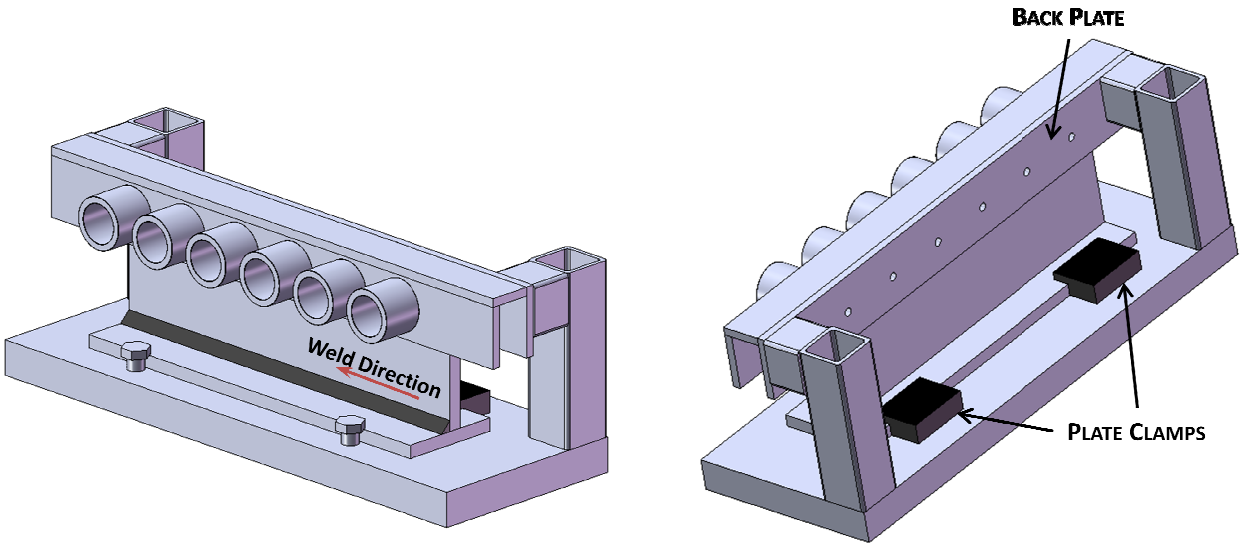

Figure 14. Weld Fixture

The vertical plate rests flat against the back before welding is performed. The back plate also serves as a machined gage block, allowing depth micrometer measurements to be taken through the holes in the back plate. The holes in the back plate correspond to the 6 spring locations. The cylindrical pieces along the front of the weld fixture hold the springs in place during welding. The cylindrical pieces are threaded to allow the springs to be tightened down against the vertical plate of the weldment. Figure 15 below shows one of the spring holders on the weld fixture.

Figure 15. Spring Holder on Weld Fixture

This weld fixture setup differs from the research done by Tsai discussed in the literature review in the location of the springs. Tsai placed spring elements at the weld joint, as can be seen in Figure 16. This research places the springs along the top of the vertical plate of the t-joint. It would be impossible to place springs at the weld joint due to accessibility issues, so the springs were placed along the top as stated.

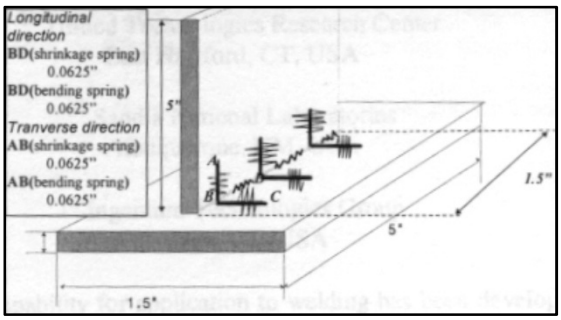

Figure 16. Tsai's spring elements [9]

Several different levels of spring restraint were tested in this experiment as shown below in Table 2. The levels were determined by using Hooke's Law with an estimate for the strength of steel at welding temperatures and at room temperatures. To determine the spring level, an estimate of the strength of low-carbon steel was acquired from Briggs [20]. From Briggs, the strength of low carbon (.15%) steel at welding temperature of approximately 700°C was estimated to be 1500 psi and for room temperature of approximately 25°C it was estimated to be 2600 psi. The cross-sectional area of the weld bead was also used to in determining the spring levels. The formula for cross-sectional area is shown in Equation 2 below.

$$A = \frac{1}{2}(LEG\ SIZE)^2 \quad (2)$$

The recommended leg size for a 3/8" plate from the handbook for arc welding is 9/32" [21]. Performing the calculation gives a cross-sectional area of the weld bead to be 0.04 square inches. Applying these values to Hooke's Law ($F = \sigma A$) gives a value of 60 pounds at welding temperature and 104 pounds at room temperature. In addition to the levels of restraint involving springs, two levels not involving spring restraint were tested. One level was welded with no springs at all and the other was a fully restrained weld with the weld pieces fully clamped down. Full restraint was achieved by inserting steel bars into the spring holders to fully restrain the weldment across the top. Spring levels were chosen to allow a spread of restraint within the calculated values.

Table 2. Summary of Weld Replications

Replication #	Spring Restraint Levels (LBS)
1-4	None
5-7	80.4
8-10	96.0
11-14	162.0
15	Full

The springs were tightened against the vertical plate, and were hence compressed by a certain length. The procedure used to tighten the springs was to do one full turn after initiating contact with the vertical plate. This resulted in roughly 0.05 inches of compression for the springs prior to welding. The spring rates for each of the levels of restraint is as follows: the 80.4 pound springs had a rate of 536 pounds per inch, the 96 pound springs had a rate of 310 pounds per inch, and the 162 pound springs had a rate of 1080 pounds per inch.

To capture the amount of distortion occurring due to the welding process, micrometer measurements were taken before the weld to get an initial position of the plate and after the weld was complete to get a final position of the plate. The difference between these two measurements is the amount of distortion. Before the final position measurements are taken, the weldments were allowed to cool to a maximum temperature of 120 °F. This was done to have consistency between each of the welds to help minimize measurement error. Each measurement was measured three times and averaged to reduce the effect of any measurement error; this average is what was reported as the distortion value for a given replication. A detailed assessment of measurement error was performed and is discussed in detail in the appendix. Measurements were also taken after the springs had been released from the part to see if there was any effect from releasing the springs. To ensure repeatability, at least 3 replications were performed at each level of spring restraint. Full restraint level was performed once to ensure that no distortion was occurring at that level. Table 2 summarizes the number of replications for each level.

The majority of the welds were performed using an automatic travel apparatus to give a consistent arc travel speed for each weld as shown in Figure 17. To further ensure that a quality weld was being produced, one specimen from each of the 5 spring levels was performed by an experienced production welder at John Deere in Ankeny, Iowa.

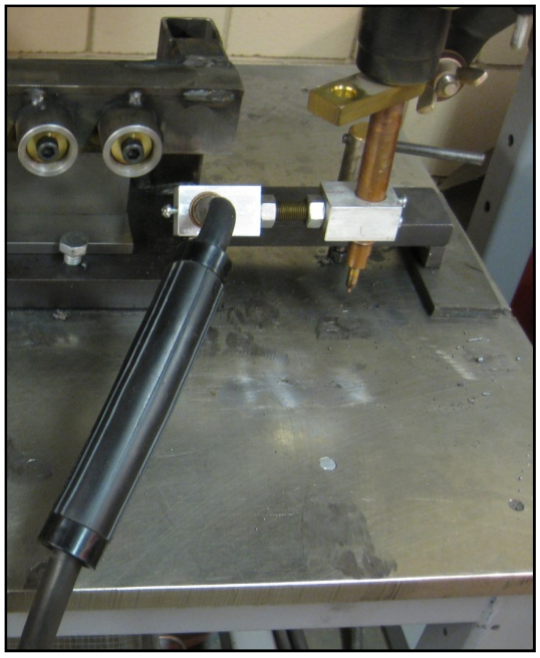

Figure 17. Automatic travel apparatus

To more fully understand the effect of the restraint on the contracting metal of the weld, residual stress measurements were performed on the welded specimens. X-ray diffraction was the method chosen to measure the residual stress in the weld specimens. A brief description of the X-ray diffraction technique is that elastic strain can be calculated from changes in interplanar spacing with the Bragg equation and wavelength of the x-ray [5].

$$\lambda = 2d\sin\theta \text{ giving } \varepsilon = \frac{\Delta d}{d} = -\cot\theta \, \Delta\theta \quad (3)$$

Once strain is determined, it can be converted into stress using a suitable value of stiffness. Two objectives were determined for the residual stress measurements. X-ray diffraction measurements were taken both parallel and perpendicular to the weld to understand the impact of restraint on the weldment. The pieces had to be prepared to fit into the x-ray diffraction machine; Figure 18 shows the size that the specimens were cut to for the x-ray diffraction tests.

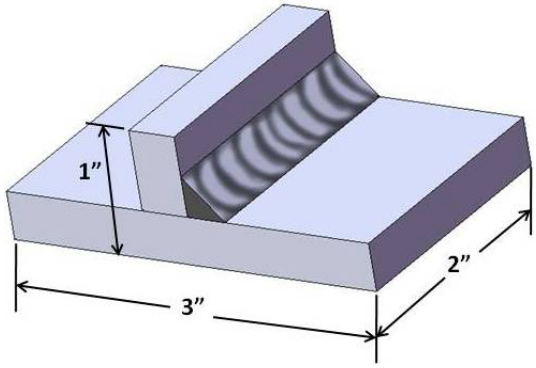

Figure 18. X-ray diffraction test piece size

It is understood that there will be some degree of stress relaxation due to the modification of the weldment by cutting it. To have a general idea of this, lines were scribed on the weldment before it was cut to allow a measurement to be taken after the piece was modified. The change in dimension due to modification was minimal, as the scribe lines were less than 1/32 of an inch different after modification by cutting. A strain gage would be necessary to determine exactly how much relaxation is occurring because of the modifications to the weldment.

For each weldment there were 24 potential measurement locations, however, due to constraints not all measurements were taken for all samples, Figure 19. In the longitudinal direction, the measurement locations are spaced every two inches, which corresponds to the spacing of the restraining springs. In the transverse direction, spacing of 5 millimeters (0.20 inches) was chosen based on previous research [17-19]. The following nomenclature is used throughout this report to designate the measurement locations (L, T) where L is the longitudinal direction from the weld start and T is the transverse direction from the center of the vertical plate, both L and T being measured in inches.

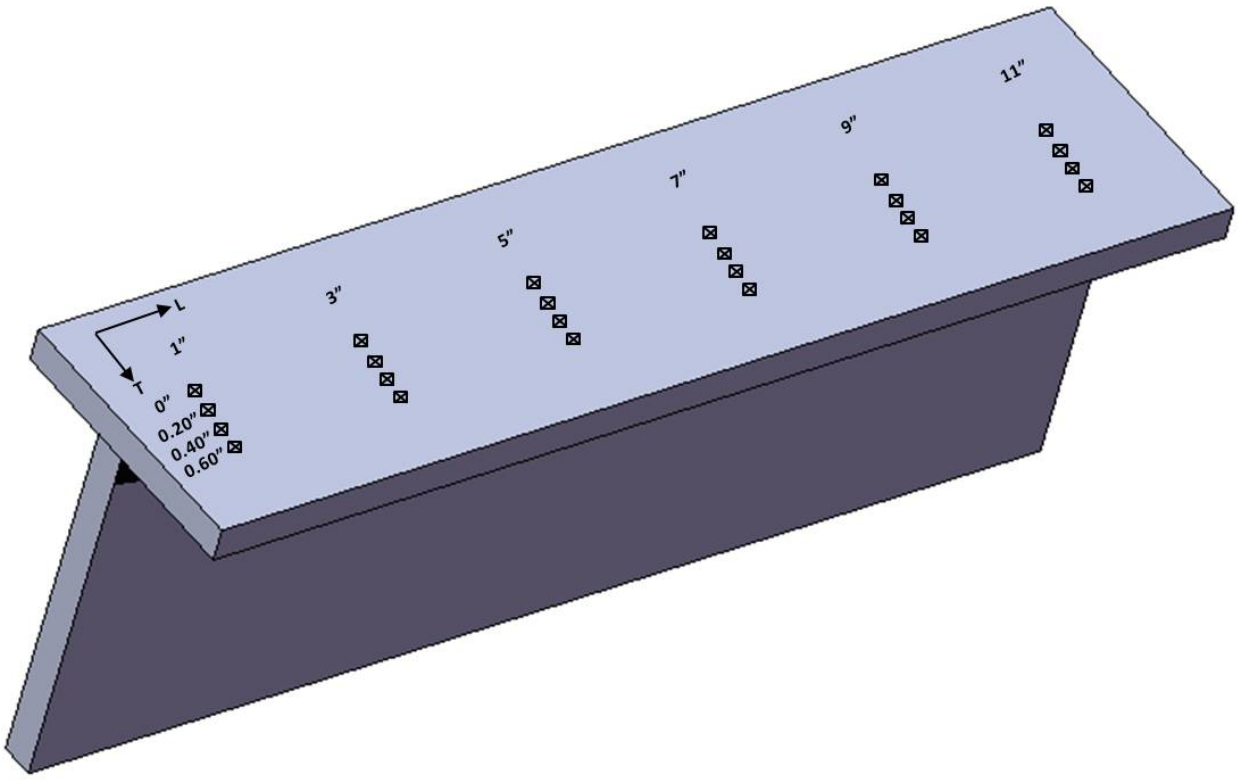

Figure 19. Stress measurement spacing

To capture the trend across the weldment, points were taken on the 96 pound specimen welded at John Deere. Points were taken at all values of L and at T = 0, 0.20, and 0.60 for a total of 18 measurement points. To capture the trend between levels of restraint, points were taken at L = 9 and L = 11 and T = 0, 0.20, 0.40 and 0.60 at each of the 5 restraint levels for a total of 30 points.

The x-ray diffraction machine used in this research was a Bruker D8 Diffractometer with a 2-dimensional aerial diffractor. The machine has a power rating of 30 kilovolts and uses chromium tubes as opposed to the more common copper tubes. The stress specimen is fixtured into the x-ray diffraction machine and the x-ray is positioned over the desired spot where the stress is to be measured. Once the x-ray is in position and the part is securely fixtured, the stress measurement direction is set into the machine. At each measurement point, the stress in the transverse direction was measured in this experiment. Transverse stress was measured because the distortion was occurring in the transverse direction. The material properties of the part are also entered in the software before the process is started. The machine requires the elastic modulus of the steel for its calculations; in this case, the modulus used was 220 GPa. Once these are set, the machine can then be turned on and the measurements can be taken. The x-ray is swept across the part to produce the diffraction peak, which the software then converts to residual stress. Figure 20 below shows how the x-ray is swept back and forth 90 degrees.

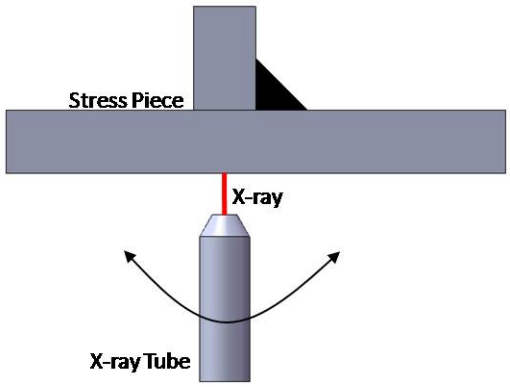

Figure 20. X-ray measurements

After the measurements are completed, the software outputs the stress values with their associated errors. Errors were never greater than ±10 MPa, with the average error being ±6 MPa.

Although no finite element modeling was done in this research, it is still important to understand some of the conditions of the experiment. Modeling the thermal aspect of the experiments would be fairly straightforward, as there are many papers on the welding heat source and its effect in finite element modeling.

The mechanical aspect of a thermo-elastic-plastic model does need to be discussed, however. Boundary conditions need to be set up to define the scope of the mechanical analysis. There are some assumptions that are made about the structure that simplify the model. They are as follows:

Assumptions

- Yielding occurs according to von Mises yield criterion and associative flow rules
- The material follows kinematic work hardening

Boundary constraints are applied on the base plate in the form of clamps. These clamps restrict the movement of the base plate in all degrees of freedom; the plate is completely restricted from movement.

The springs across the top of the vertical plate also need to be considered. The spring restraint is not full restraint in all directions as the clamps are. The main goal of the springs is to restrain distortion in the direction transverse to the weld line. Therefore, the springs only restrict the vertical plate from moving in one direction, allowing the plate to possibly slide in the other two directions.

Another consideration in modeling the spring restraint is the fact that the springs are applying different amounts of force at different points in time. This means that the spring restraint must be modeled as a transient model.

Chapter 4. Results

This section presents the distortion and residual stress data collected from the experiment performed. The distortion data will be presented followed by the residual stress data acquired from the x-ray diffraction software. Weld bead quality will also be presented to confirm that the weld settings used in the experiment were producing quality welds.

Figure 21 shows the results from all the weldments performed in the experiment. The horizontal axis corresponds to measurement points taken along the length of the weld at a distance from the start of the weld, denoted by L. The welds with no springs were tack welded on each end to hold the vertical piece in place, so the piece was not exactly vertical after the tacks were placed. The initial measurements were taken after the tack welds were in place. The data for the welds with no springs was very inconsistent. The data for the three levels of spring restraint was very consistent, with a good agreement between the welds performed with the automatic travel table and the welds done at John Deere. It should be noted that the 80.4 pound springs do not completely prevent distortion at the beginning of the weld, still allowing 0.01-0.02 inches of distortion. Also, a gradual increase in distortion is seen as the distance from the start of the weld increases.

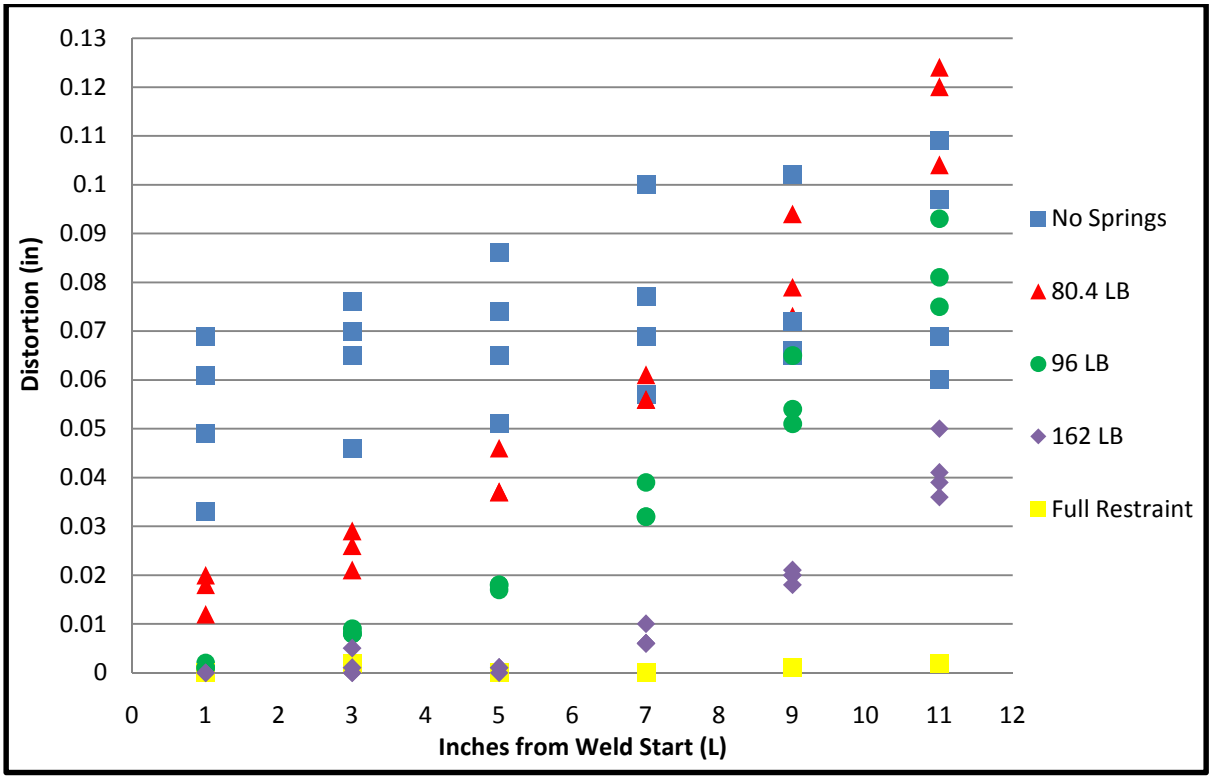

Figure 21. Distortion data for all welds

The 96 pound springs hold the piece to no distortion at L = 1 and experience the same gradual increase in distortion as L increases. The highest spring restraint of 162 pounds held the piece to no distortion from L = 0 to L = 5. The 162 pound restraint weldments seem to experience a sharper increase in distortion because the distortion is only occurring in the second half of the weld specimens, but the overall distortion is the lowest of the three spring restraint levels. Steel rods were placed in the spring holders to achieve full restraint of the weldment. The full restraint weld was performed at John Deere and has good agreement with the zero distortion to be expected from a fully restrained weld as can be seen in Figure 21.

Figure 22 shows the effect of different levels of spring restraint. As can be seen, as the spring restraint increases the distortion experienced decreases. An average distortion experienced for each level of spring restraint was taken at L = 11 to compare and is denoted by a line in Figure 22. The average value for the weld specimens with no spring restraint ended up being lower than the 80.4 pound spring restraint value. This can be attributed to the tack welds that were required to hold the vertical piece; these tacks had an effect on where the weld piece was initially located, possibly providing restraint to the weldment.

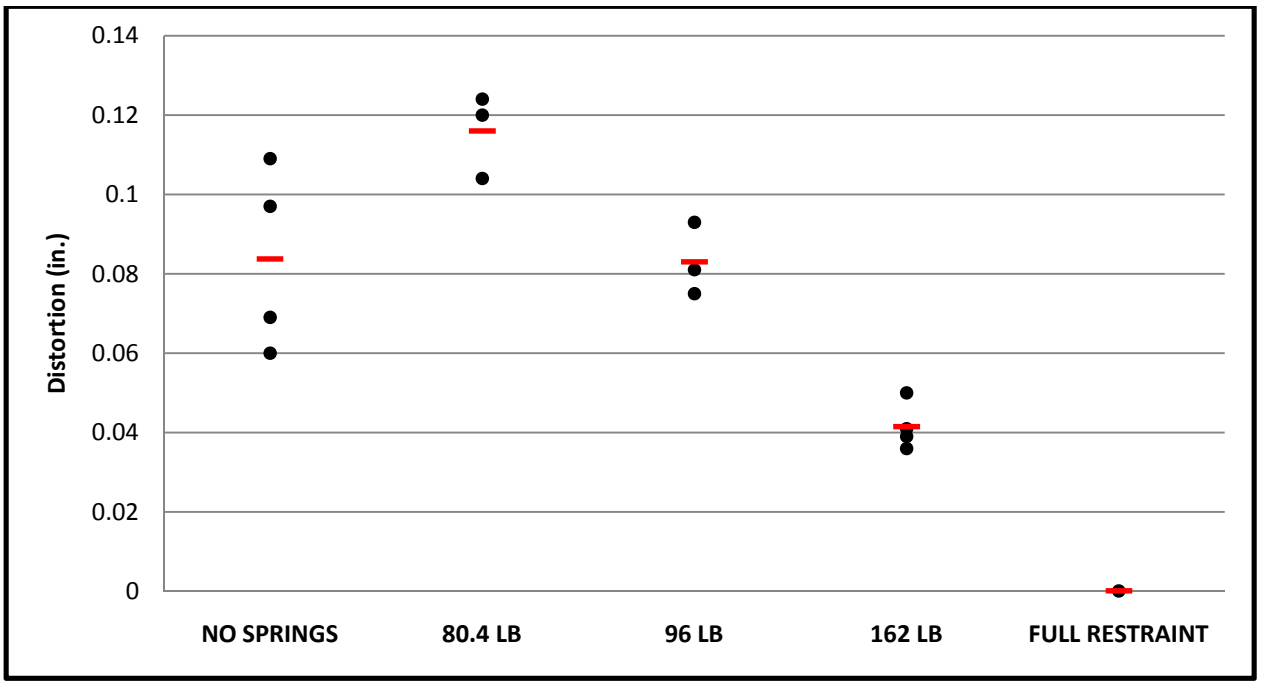

Figure 22. Distortion data for each spring restraint level at L = 11

A weldment was also produced to see the effect of the tack welds on the weldments with no spring restraint. Figure 23 below shows the distortion data for a weldment produced with one tack weld located at the beginning of the weld. As can be seen, the distortion is much greater on this weldment that the other weldments with no spring restraint and two tack welds. This confirms that the tack weld located at the end of the weld is most certainly providing a degree of restraint.

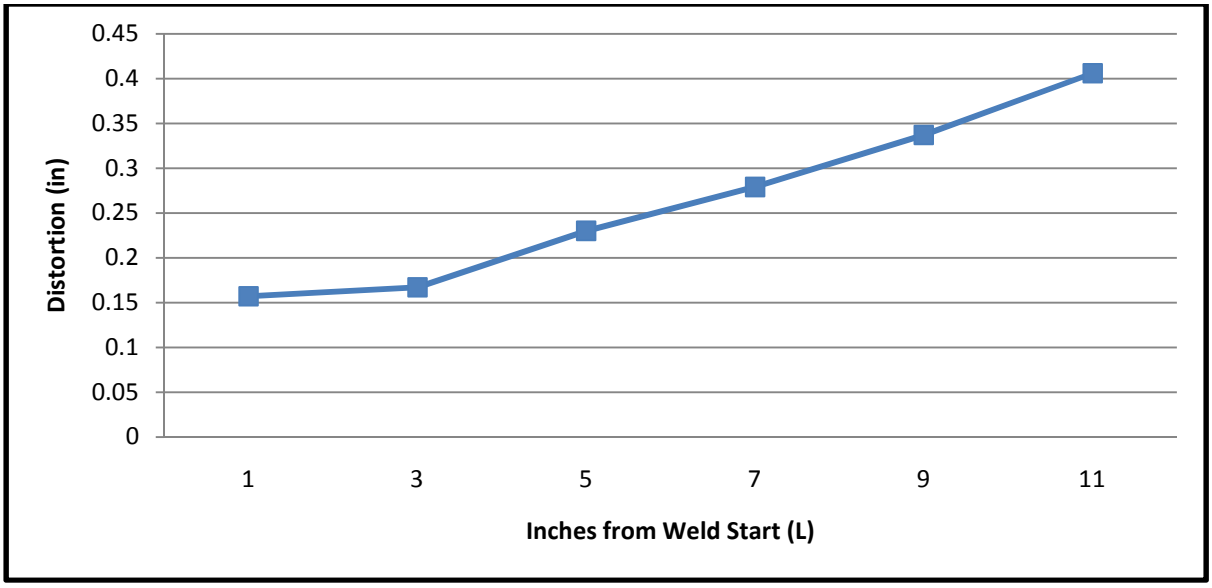

Figure 23. Distortion data for weldment with no spring restraint and one tack weld

Figure 24 shows the distortion data for the weldments performed at John Deere. This graph is presented to help show the relationship between distortion and residual stress, which will be presented in Figures 25-28.

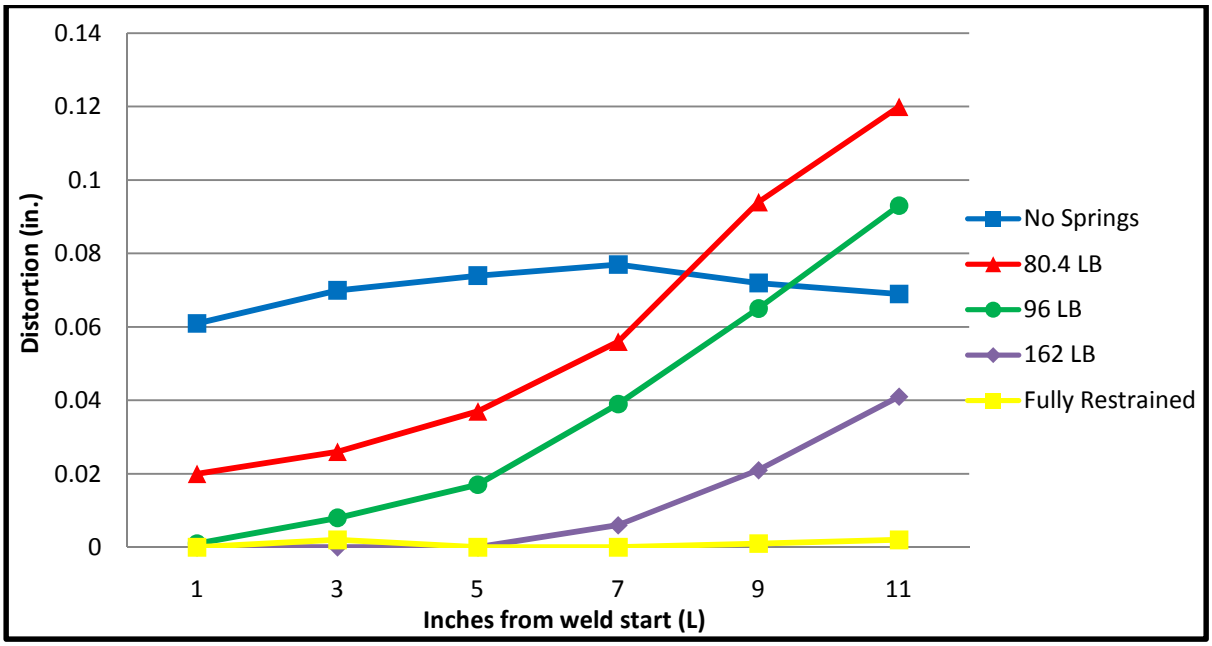

Figure 24. Distortion data for welds performed at John Deere

Figure 25 shows the residual stress data at T = 0 for the weldments performed at John Deere for each of the restraint levels. The stress experienced is tensile stress, and is fairly consistent across the weldment. The stress values for the welds with springs show lower stress values than for the unrestrained weld.

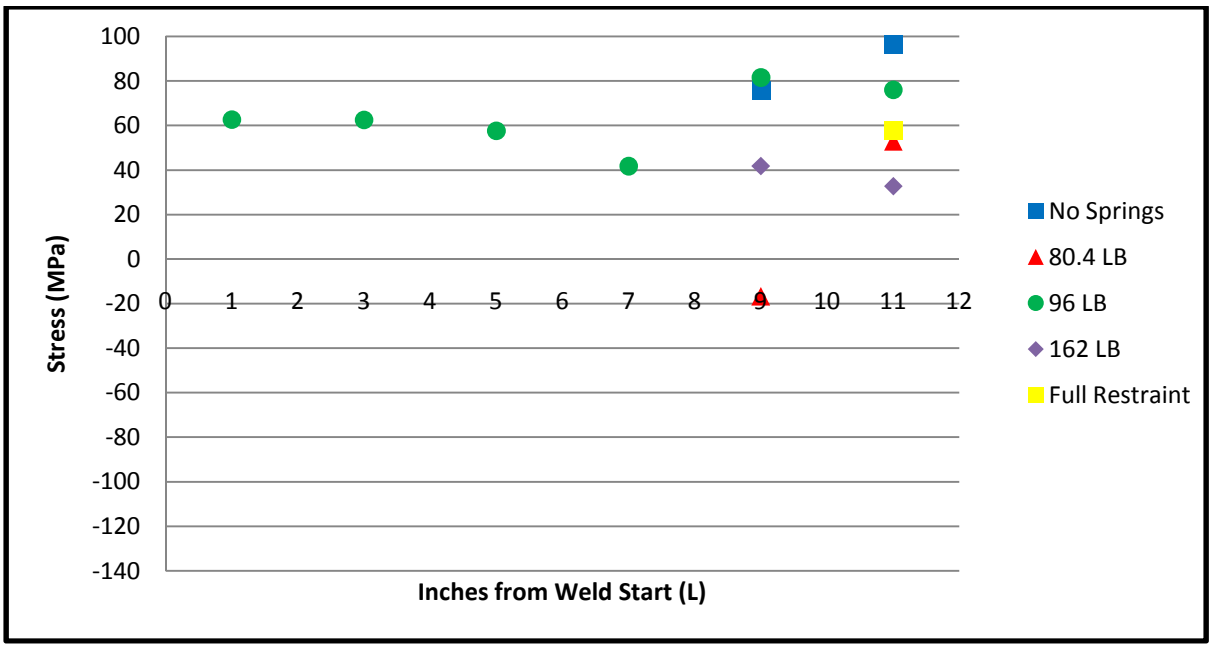

Figure 25. Residual stress data at T = 0 for welds performed at John Deere

Figure 26 shows the residual stress data at T = 0.20 for the weldments performed at John Deere for each of the restraint levels. The trend across the weldment starts out as tensile stress at the beginning of the weld and transitions to compressive stress roughly at the middle of the weld. The springs show a lower stress value at the end of the weld than the weldments with no restraint and full restraint.

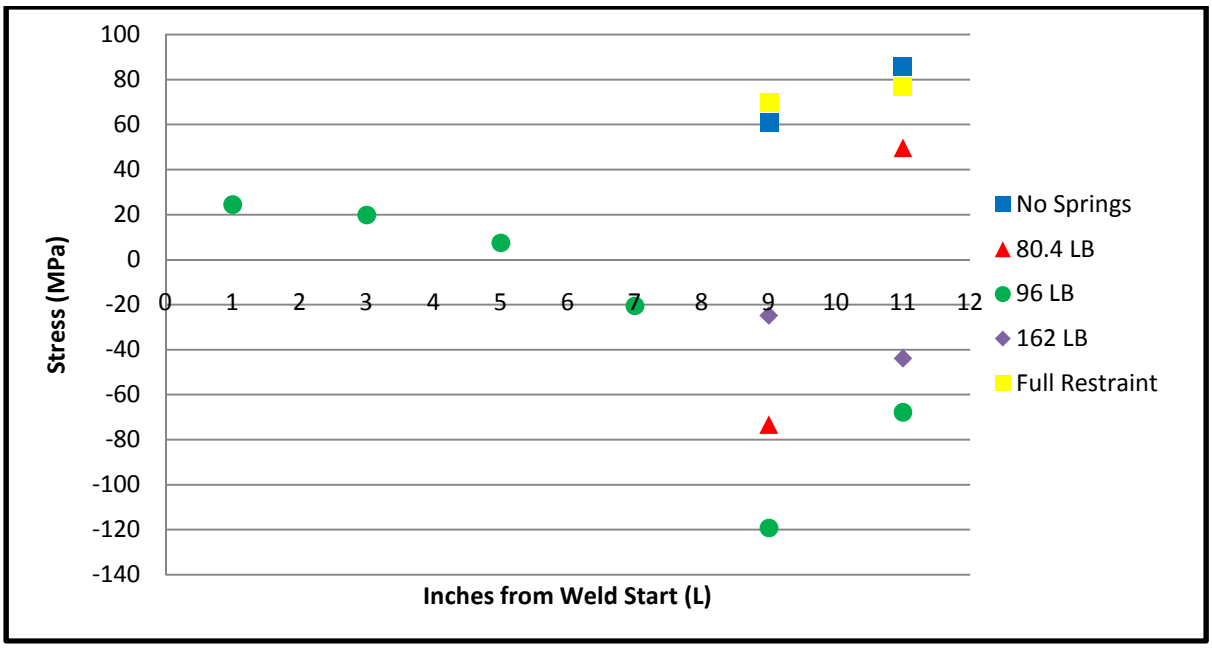

Figure 26. Residual stress data at T = 0.20 for welds performed at John Deere

Figure 27 shows the residual stress data at T = 0.40 at L = 11 for the weldments performed at John Deere for each of the restraint levels. The stress values for the welds with springs show lower stress values than for the unrestrained weld.

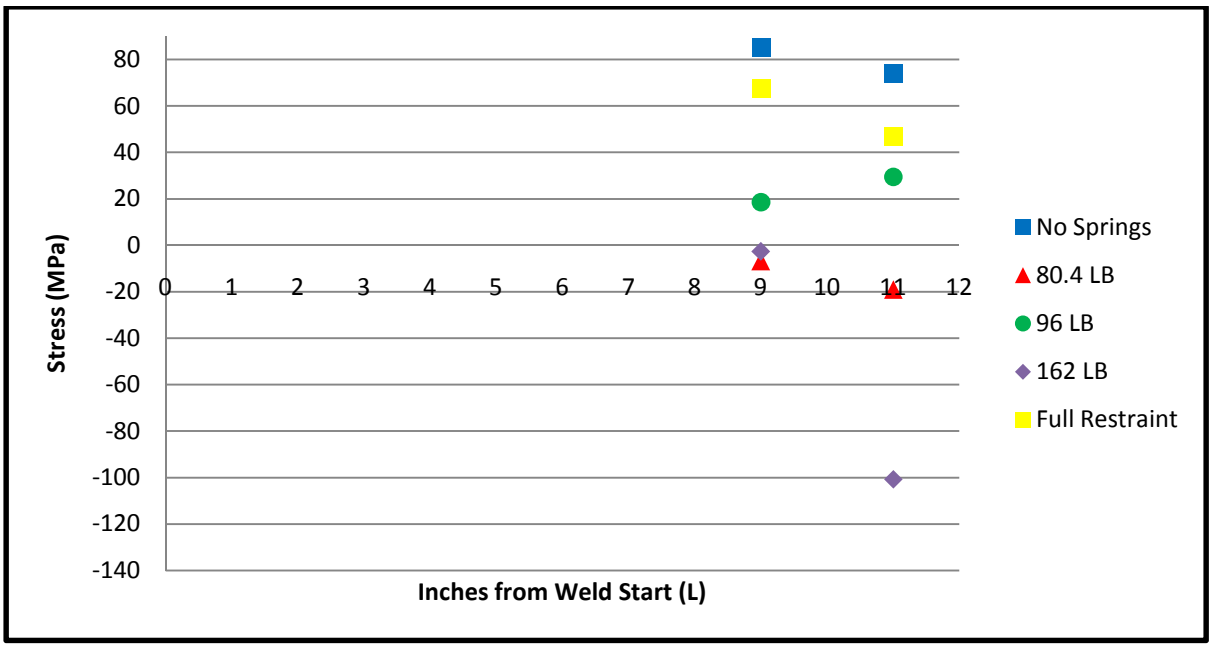

Figure 27. Residual stress data at T = 0.40 for welds performed at John Deere

Figure 28 shows the residual stress data at T = 0.60 for the weldments performed at John Deere for each of the restraint levels. The trend across the weldment starts out as tensile stress at the beginning of the weld stays tensile for the most part with the exception at T = 9 where compressive stress is experienced. The springs show a lower stress value at the end of the weld than the weldment with full restraint.

Figure 28. Residual stress data at T = 0.60 for welds performed at John Deere

4.1 Size and Shape of the Weld Bead

It is also important to verify that the welds that were performed are considered to be quality welds. A full strength weld is designed according to the leg size of the weld [21]. The weld leg size, ω, is defined as three quarters of the thickness of the plates being welded (ω = ¾t). In this research, to acquire a full strength weld, a weld leg size of at least 0.28125 inches is needed. The leg size of a weld can be determined by the largest right triangle that can be inscribed within the weld cross-section. A diagram demonstrating this can be seen below in Figure 29.

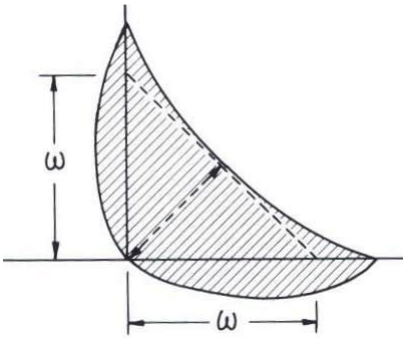

Figure 29. Determination of weld leg size, ω [21]

In order to determine if the weld settings were producing a quality weld, two samples were chemically etched with standard etching procedures and a 15% nitric acid 85% methanol etching solution to reveal the cross-section of the weld bead. Samples etched were the 96 pound weld produced at John Deere at L=1 and L = 11. Figure 30 below shows the cross-section of the 96 pound weld at L = 1 with the inscribed triangle to determine the weld leg size. From the triangle, the weld leg size at L = 1 is approximately 0.33 inches. The maximum depth of the weld is approximately 0.254 inches.

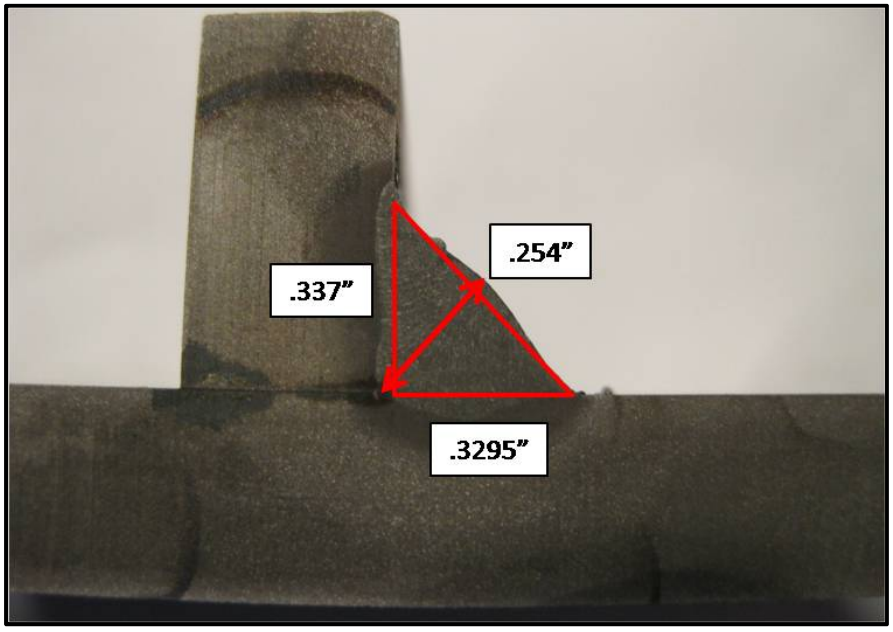

Figure 30. Cross-section of 96 pound weld at L = 1

Figure 31 below shows the cross-section of the 96 pound weld at L = 11 with the inscribed triangle to determine the weld leg size. From the triangle, the weld leg size at L = 11 is approximately 0.34 inches. The maximum depth of the weld is approximately 0.310 inches.

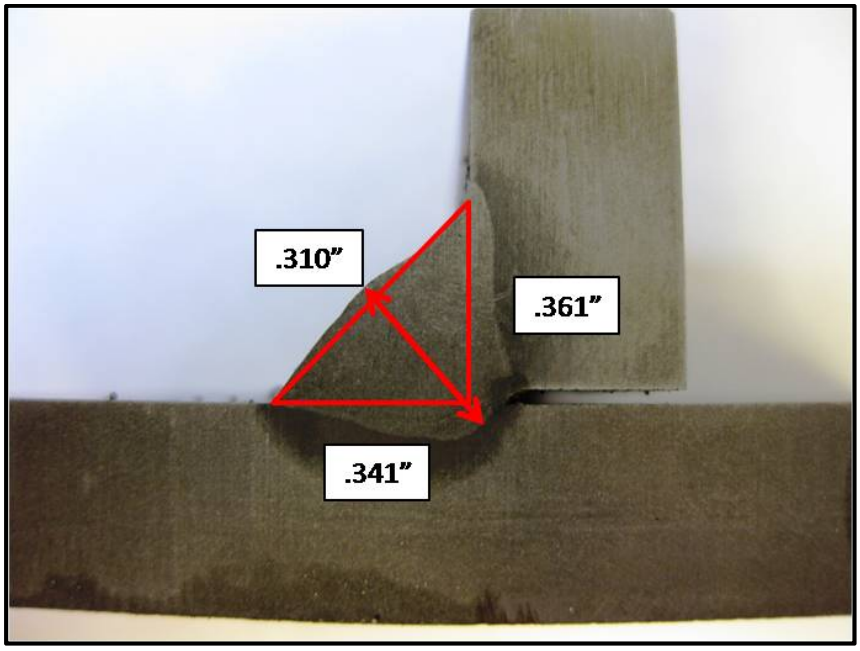

Figure 31. Cross-section of 96 pound weld at L = 11

Both of the etches confirm that the weld settings are producing a weld that meets the specification for the minimum weld leg size of 0.28125 inches required to be considered a full strength weld.

Chapter 5. Discussion

This discussion section provides an opportunity to explain some of the trends and data from the results of the experiments. The first topic discusses the distortion data patterns and why they follow a longitudinal bending distortion pattern. Lastly, the trends associated with residual stress data will be discussed.

5.1 Distortion Data Pattern

The distortion data pattern for the weldments with spring restraint can be explained by longitudinal contraction forces. The distortion follows a longitudinal bending pattern from little to no distortion at the beginning of the weld to a significant amount at the end of the weld. Longitudinal contraction forces give rise to longitudinal bending and the deviation of the weldment is intensified by these contraction forces, increasing in a non-linear manner as weld is added to the structure [22]. Energy across the weld is also increasing as more weld metal is added to the structures, and this higher energy input will lead to distortion. This means at the beginning of the weld, the contraction force is not large enough to overcome the restraint provided by the springs, and the result is little to no distortion at the beginning of the weld. In contrast, at the end of the weld, the contraction force has been increasing in a non-linear manner and the energy has been building up as well as the weld is added to the t-joint. The buildup of energy and contraction force is enough to overcome the restraint provided by the springs at the end of the weldment. The result of this is that there is a significant amount of distortion experienced by the weldments at the end of the weld.

5.2 Residual Stress Trends

In the residual stress data, there is a trend as L increases. The stress data that is taken at T = 0.20 starts out as tensile stress at the beginning of the weld and transitions to compressive stress roughly halfway through the weld pass (L = 6), as can be seen in Figure 32 below. This phenomenon can be partially explained by the heating and cooling of the weld pool. Upon heating, the weld pool and heat-affected zone (HAZ) expand resulting in a residual compressive stress in the weld and a residual tensile stress in the base metal [23]. Normally, as the weldment solidifies and cools, the weld pool volume contracts, leaving a tensile stress in the weld and a compressive stress in the base metal. The weld metal is in tensile stress at the beginning of the weld, which can be attributed to a combination of several things. At the beginning of the weld, there is little to no distortion, meaning that the vertical plate is not moving. Also, there is a small amount of energy from heat input at the beginning of the weld since the heat has not had a chance to build up. Combining these things means that the spring restraint is larger than the contraction force and energy, holding the plate to no distortion. This can explain the tensile stress at the beginning of

the weldment being tensile; it has been locked-in because of the weld metal trying to contract but not being able to do so.

Figure 32. Stress pattern, 96 pound John Deere weld at T = 0.20

Near the middle of the weldment, there is an area that is experiencing no stress. To explain this, the concept of reaction stress needs to be introduced. Reaction stresses are stresses that are caused by external constraints to the system [24]. These reaction stresses are caused by the distortion of the vertical plate causing the plate to push against the weld metal. The spring restraint is no longer fully restraining the vertical plate from moving, allowing the plate to distort. This action of the plate pushing on the weld metal causes a compressive reaction stress which grows as more distortion occurs. By the middle of the weldment, the compressive reaction stress is roughly equivalent to the usual tensile stress that is locked-in the weld from restrained contraction. Stresses add vectorially, meaning that adding a tensile stress and a compressive stress of the same magnitude essentially leads to a zero stress, which is what is seen at the middle of the weldment. By the end of the weldment, the reaction stress caused by the distortion and built up energy has grown much larger than the spring restraint, and the compressive stress overtakes the tensile stress. This leaves a compressive stress at the end of the weld as seen in Figure 32.

Chapter 6. Conclusions

This research uses spring restraint resisting the contraction of the weld metal to help understand what is happening in the weld metal in one-sided t-joint fillet welds. The results of this research begin to present some insight into the concept of variable restraint. The weld settings that were chosen were providing quality welds as was shown by the etching procedure.

The distortion pattern produced from the welds that had spring restraint acting upon them followed a longitudinal bending distortion pattern. This result provided insight into realizing that the contraction forces and energy were growing non-uniformly as more weld was being added to the weldment. Using one level of spring restraint across the weldment seems to be insufficient to hold the weldment to minimal distortion, as even the larger springs did not achieve zero distortion.

The residual stress data can begin to be explained by the concept of reaction stresses. However, it should be noted that the stress distributions are a very complex entity and this explanation is by no means a complete and definitive explanation of what is going on with the residual stress patterns in these weldments.

Chapter 7. Future Work

There is good potential for future work that can be extended from this project. The first area that can be explored would be to complete the entire set of residual stress data for every restraint level. This could give more insight into exactly what is going on in the different levels of restraint. X-ray diffraction is an expensive process and was a limiting factor in this research.

Another area of focus for future work would be to investigate spring restraint levels above 162 pounds. The 162 pound springs still did not keep the weldment to a reasonable level of distortion at the end of the weld, so investigating higher levels of restraint would be beneficial to see if the restraint levels are becoming too high and leave residual stresses in the weldment, i.e. they are acting like a fully restrained weldment. This work would be instrumental in determining if variable restraint can possibly reduce both distortion and stress.

The final area that could be investigated concerns the restraint across the weldment. In this research, the springs were kept constant across the weldment. From the results obtained, it would be useful to consider the effects of using different levels of restraint across the weld. This would be done by mixing the springs across the weldment, most likely starting with lower values of restraint and transitioning along the weldment to higher levels at the end of the weld. This is basically the concept of variable restraint; doing an experiment such as this would unveil if variable restraint across the weldment can indeed reduce distortion while reducing stress.

Appendix A. Measurement Error Analysis

Repeatability is the variation in measurements taken by one person or instrument on the same item and under the same conditions. Repeatability can also be thought of as precision of a measurement instrument. In these experiments, every measurement was performed by one operator, so repeatability is the main possible source of error.

To quantify the repeatability error, multiple trials and parts as needed. In this error analysis, a total of 6 different "parts" were measured. Parts in this analysis refer to each of the 6 measurement positions on the gage block of the weld fixture. The number of measurements taken at each position, or number of trials, was 10 at each position. All measurements were done on a part that was completely restrained against the gage block.

The measurement system repeatability is:

$$Repeatability = \frac{5.15\bar{\bar{R}}}{d_2}$$

where $\bar{\bar{R}}$ is the average range for all positions and trials, and

d_2 is found from Table 1 with Z = number of parts times number of appraisers,

and W= number of trials.

Table 1: Values of d_2

z	w													
	2	3	4	5	6	7	8	9	10	11	12	13	14	15
1	1.41	1.91	2.24	2.48	2.67	2.83	2.96	3.08	3.18	3.27	3.35	3.42	3.49	3.55
2	1.28	1.81	2.15	2.40	2.60	2.77	2.91	3.02	3.13	3.22	3.30	3.38	3.45	3.51
3	1.23	1.77	2.12	2.38	2.58	2.75	2.89	3.01	3.11	3.21	3.29	3.37	3.43	3.50
4	1.21	1.75	2.11	2.37	2.57	2.74	2.88	3.00	3.10	3.20	3.28	3.36	3.43	3.49
5	1.19	1.74	2.10	2.36	2.56	2.78	2.87	2.99	3.10	3.19	3.28	3.36	3.42	3.49
6	1.18	1.73	2.09	2.35	2.56	2.73	2.87	2.99	3.10	3.19	3.27	3.35	3.42	3.49
7	1.17	1.73	2.09	2.35	2.55	2.72	2.87	2.99	3.10	3.19	3.27	3.35	3.42	3.48
8	1.17	1.72	2.08	2.35	2.55	2.72	2.87	2.98	3.09	3.19	3.27	3.35	3.42	3.48
9	1.16	1.72	2.08	2.34	2.55	2.72	2.86	2.98	3.09	3.19	3.27	3.35	3.42	3.48
10	1.16	1.72	2.08	2.34	2.55	2.72	2.86	2.98	3.09	3.18	3.27	3.34	3.42	3.48
11	1.15	1.71	2.08	2.34	2.55	2.72	2.86	2.98	3.09	3.18	3.27	3.34	3.41	3.48
12	1.15	1.71	2.07	2.34	2.55	2.72	2.85	2.98	3.09	3.18	3.27	3.34	3.41	3.48
13	1.15	1.71	2.07	2.34	2.55	2.71	2.85	2.98	3.09	3.18	3.27	3.34	3.41	3.48
14	1.15	1.71	2.07	2.34	2.54	2.71	2.85	2.98	3.09	3.18	3.27	3.34	3.41	3.48
15	1.15	1.71	2.07	2.34	2.54	2.71	2.85	2.98	3.08	3.18	3.26	3.34	3.41	3.48
>15	1.128	1.693	2.059	2.326	2.534	2.704	2.847	2.97	3.078	3.173	3.258	3.336	3.407	3.472

For this experiment, Z was equal to 6 (6 positions times 1 appraiser) and W was equal to 10 (10 trials). This led to a value of d_2 of 3.10.

Table 2 below shows the data acquired for the error experiment. R for each row is the calculated range for that position across the 10 trials. $\bar{\bar{R}}$ is the average of all the ranges across the 6 positions.

Table 2: Measurement error data

	TRIAL										
POSITION	1	2	3	4	5	6	7	8	9	10	R
1	0.249	0.25	0.249	0.25	0.249	0.249	0.249	0.25	0.25	0.249	0.001
2	0.25	0.25	0.25	0.251	0.251	0.25	0.25	0.251	0.25	0.251	0.001
3	0.248	0.248	0.248	0.249	0.248	0.248	0.248	0.249	0.249	0.248	0.001
4	0.247	0.247	0.248	0.248	0.247	0.247	0.248	0.247	0.248	0.248	0.001
5	0.249	0.25	0.25	0.25	0.249	0.25	0.249	0.25	0.25	0.249	0.001
6	0.25	0.251	0.25	0.25	0.251	0.25	0.251	0.251	0.25	0.251	0.001
										$\bar{\bar{R}}$	**0.001**

From this data, calculating the repeatability for this measurement process is shown below.

$$Repeatability = \frac{5.15 * 0.001}{3.10} = 0.00166$$

So from this measurement error analysis, it can be said that the measurement system is repeatable to 0.00166 inches, which is an acceptable error.

Formula and Table 1 acquired from following reference.

Repeatability and Reproducibility. Publication. 1999. Engineered Software, Inc. <http://www.engineeredsoftware.com/papers/msa_rr.pdf>.

References Cited

[1] Groover, Mikell P. Fundamentals of Modern Manufacturing : Materials, Processes, and Systems. New York: John Wiley & Sons Australia, Limited, 2001.

[2] Sluzalec, Andrzej. “Theory of Thermomechanical Processes in Welding.” New York: Springer, 2005.

[3] Masubuchi, K. "In-Process Control and Reduction of Residual Stresses and Distortion in Weldments." Proc. of Practical Applications of Residual Stress Technology, Indianapolis, IN. 1991.

[4] Kumose, T., T. Yoshida, T. Abe, and H. Onoue. "Prediction of Angular Distortion Caused by One-Pass Fillet Welding." Welding Journal (1954): 945-956.

[5] Withers, P. J., and H. Bhadeshia. "Residual stress Part 1 – Measurement techniques." Materials Science and Technology 17 (2001): 355.

[6] Rosenthal, D. “Mathematical theory of heat distribution during welding and cutting.” Welding Journal 20 (1941): 220-s to 234-s.

[7] Goldak, John, Aditya Chakravarti, and Malcolm Bibby. “A New Finite Element Model for Welding Heat Sources.” Metallurgical Transactions B 15B (1984): 299-305.

[8] Nguyen, N.T., Ohta, A. Matsuoka, K., Suzuki, N. and Maeda, Y. “Analytical solutions for transient temperature of semi-infinite body subjected to 3-D moving heat sources.” Welding Journal, Aug. 1999: 265s to 274s.

[9] Tsai, C., W. Cheng, and H. Lee. “Modelling Strategy for Control of Welding-Induced Distortion.” Proc. of Modeling of Casting, Welding and Advanced Solidification Processes VII, London, England. (1995): 335-345.

[10] Mahapatra, M., G. L. Datta, B. Pradhan, and N. R. Mandal. “Modelling the effects of constraints and single axis welding process parameters on angular distortions in one-side fillet welds.” Proc. IMechE 221 Part B: 397-407.

[11] Kumose, T., T. Yoshida, T. Abbe, and H. Onoue. “Prediction of Angular Distortion Caused by One-Pass Fillet Welding.” Welding Journal. 1954: 945-956.

[12] Michaleris, P., J. Dantiz, and D. Tortorelli. "Minimization of welding residual stress and distortion in large structures." Welding Journal 11 (1999): 361-366s.

[13] Okerblom, N.O. "The Calculations of Deformations of Welded Metal Structures." 1958 (Her Majesty’s Stationery Office, London).

[14] Camilleri, D., T. Comlekci, and T. Gray. "Computational prediction of out-of-plane welding distortion and experimental investigation." The Journal of Strain Analysis for Engineering Design 40 (2005): 161-176.

[15] Teng, T., and C. Lin. “Effect of welding conditions on residual stresses due to butt welds.” International Journal of Pressure Vessels and Piping 75 (1998): 857-864.

[16] Teng, T., C. Fung, P. Chang, and W. Yang. *Analysis of Residual Stresses and Distortions in T-Joint Fillet Welds*. International Journal of Pressure Vessels and Piping 78 (2001): 523-538.

[17] Tekriwal, P., and J. Mazumder. "Transient and Residual Thermal Strain-Stress Analysis of GMAW."Journal of Engineering Materials and Technology 113 (1991): 336-343.

[18] Andersson, B. "Thermal Stresses in a Submerged-Arc Welded Joint Considering Phase Transformations."Journal of Engineering Materials and Technology 100 (1978): 356-362.

[19] Wimpory, R., P. May, N. O'Dowd, G. Webster, D. Smith, and E. Kingston. "Measurement of residual stresses in T-plate weldments." Journal of Strain Analysis 38 (2003): 349-365.

[20] Briggs, C. and R. Gezelius. “Studies on the Solidification and Contraction in Steel Castings II – Free and Hindered Contraction of Cast Carbon Steel, Transactions.” American Foundrymen’s Association 42 (1934): 449-470.

[21] Procedure Handbook of Arc Welding. Boston: Lincoln Electric Company, 1994.

[22] Mollicone, P., D. Camilleri, T. Gray, and T. Comlekci. "Simple thermo-elastic–plastic models for welding distortion simulation." Journal of Materials Processing Technology 176 (2006): 77-86.

[23] Feng, Zhili. Processes and mechanisms of welding residual stress and distortion (Woodhead Publishing in Materials). CRC, 2005: p 4.

[24] Welding Handbook. Miami, FL: American Welding Society, 1987.